



U.S. Department
of Transportation
**National Highway
Traffic Safety
Administration**



DOT HS 812 105

December 2014

Characterizing Child Head Motions Relative to Vehicle Rear Seat Compartment in Motor Vehicle Crashes

DISCLAIMER

This publication is distributed by the U.S. Department of Transportation, National Highway Traffic Safety Administration, in the interest of information exchange. The opinions, findings, and conclusions expressed in this publication are those of the authors and not necessarily those of the Department of Transportation or the National Highway Traffic Safety Administration. The United States Government assumes no liability for its contents or use thereof. If trade or manufacturers' names or products are mentioned, it is because they are considered essential to the object of the publication and should not be construed as an endorsement. The United States Government does not endorse products or manufacturers.

Suggested APA Format Citation:

Hu, J., Klinich, K. D., Reed, M. P., Ebert-Hamilton, S. M., & Rupp, J. D. (2014, December). *Characterizing child head motions relative to vehicle rear seat compartment in motor vehicle crashes*. (Report No. DOT HS 812 105). Washington, DC: National Highway Traffic Safety Administration.

Technical Report Documentation Page

1. Report No. DOT HS 812	2. Government Accession No.	3. Recipient's Catalog No.	
4. Title and Subtitle Characterizing Child Head Motions Relative to Vehicle Rear Seat Compartment in Motor Vehicle Crashes		5. Report Date December 2014	
		6. Performing Organization Code	
7. Author(s) Hu, Jingwen; Klinich, Kathleen D.; Reed, Matthew P.; Ebert-Hamilton, Sheila M.; Rupp, Jonathan D.		8. Performing Organization Report No. UMTRI-2012-20	
9. Performing Organization Name and Address University of Michigan Transportation Research Institute 2901 Baxter Rd. Ann Arbor MI 48109		10. Work Unit No. (TRAIS)	
		11. Contract or Grant No.	
12. Sponsoring Agency Name and Address National Highway Traffic Safety Administration 1200 New Jersey Avenue SE. Washington, DC 20590		13. Type of Report and Period Covered April 2011 to July 2012	
		14. Sponsoring Agency Code	
15. Supplementary Notes			
16. Abstract <p>Improved padding or other countermeasures in vehicle rear compartments could reduce the incidence of head trauma for child occupants. However, knowledge of likely child head impact locations for a range of crash scenarios is needed to determine which areas and structures should be padded and where a side curtain should be deployed to protect child occupants. The objective of this study is to use a scalable MATHematical DYnamic MOdels (MADYMO) model of a child occupant to estimate the distributions of possible head impact locations as a function of crash type, vehicle interior characteristics, and child size. To achieve this goal, a series of simulations using a scalable MADYMO child-ATD model was conducted. The geometries of the second-row compartment from 5 vehicles were recorded using a laser scanner to provide high-resolution data for assessing probable head contact zones. Distributions of lateral and longitudinal delta V were calculated as a function of PDOF using the NASS-CDS dataset to provide proper simulation conditions based on real-world crashes. Simulations of crashes ranging from pure frontal to pure side impact (9 o'clock to 3 o'clock) with child ATDs with and without backless boosters were conducted using UMTRI's parametric child ATD model in MADYMO, UMTRI's child ATD positioning procedure, and UMTRI's automated belt-fit and crash simulation system. The simulation results were used to create a model of the spatial distribution of head trajectories based on child body size and crash direction. By combining the head motion model and the vehicle second-row geometry models, the likely head contact zones with respect to interior components were identified. The findings of this study provide a reference for future vehicle rear compartment design to reduce head injuries for older children.</p>			
17. Key Word Rear seat, Older children, Side impact, Child head motion, Computer simulation		18. Distribution Statement Document is available to the public from the National Technical Information Service www.ntis.gov	
19. Security Classif. (of this report) None	20. Security Classif. (of this page) None	21. No. of Pages 34	22. Price

Acknowledgments

This work was funded by the National Highway Traffic Safety Administration under cooperative agreement DTNH22-10-H-00288 with the University of Michigan. The opinions expressed herein are those of the authors and do not necessarily represent those of the funding agencies.

Table of Contents

List of Figures	iv
List of Tables	v
1 Introduction	1
2 Methods	3
2.1 Vehicle Scan Procedure	3
2.2 ATD Model Development and Validation	4
2.3 Crash Conditions	6
2.4 Simulation Matrix	8
2.5 Automated Simulation Procedure	9
2.6 Head Contact Zones	10
3 Results	11
3.1 Vehicle Scans	11
3.2 Vehicle Crash Pulse	12
3.3 Simulated Head Trajectories Compared to Vehicle Second-Row Geometry	14
3.4 Head Trajectory as a Function of Delta V	20
4 Discussion	21
4.1 Comparing to Previous Studies in Terms of Head Contact Zones	21
4.2 Seat Belt and Booster Seat Effectiveness in Reducing Injuries for Children	22
4.3 Implications for Vehicle Countermeasures	23
4.4 Limitations and Future Work	23
5 Summary	24
6 References	25

List of Figures

Figure 1: FARO Arm shown mounted to a vehicle (left) and being used to digitize the shape of vehicle pillar (right) in a grid pattern.....	3
Figure 2: Measuring the location of the rear seat H-point	4
Figure 3: Fusion FARO arm with laser scanner attached	4
Figure 4: Baseline Hybrid III 6YO ATD model (Wu et al., 2012)	4
Figure 5: Comparison between real seat cushion and seat cushion model (bottom view).	5
Figure 6: Seating postures of ATDs with different body sizes in vehicle seat and booster.....	6
Figure 7: Distribution of crashes by PDOF. Numbers indicate clock direction and percentage of all planar crashes.	7
Figure 8: Simulated delta V	7
Figure 9: ModeFrontier flowchart for setting up the automated simulations	10
Figure 10: Scanned vehicle second-row environment geometry.....	11
Figure 11: Comparison of crash pulses between Side-NCAP and FMVSS No. 214 side impact tests	13
Figure 12: Comparison of scaled crash pulses between FMVSS No. 213 test and vehicle side impact tests	14
Figure 13: Head top trajectories of simulated child ATDs with and without booster seats.....	15
Figure 14: Head top trajectories of simulated child ATDs with different delta V	20
Figure 15: Comparison of head contact zone between the Maltese study and simulated contacts for 6- to 8-, 9- to 10-, and 11- to 12-year-old children in the current study	22

List of Tables

Table 1: Key percentiles value of delta V (km/h) for each crash mode.	7
Table 2: Distributions of variables in the parametric study.....	9
Table 3: Head top trajectories of child occupants with (yellow) and without (red) booster seats overlaid in the Audi A4 second-row geometry.....	17
Table 4: Head top trajectories of child occupants with (yellow) and without (red) booster seats overlaid in the Toyota Sienna second-row geometry	18
Table 5: Head top trajectories of child occupants (yellow) and without (red) booster seats overlaid in the Saturn Vue second-row geometry	19

1 Introduction

Although improvements in child passenger safety have reduced the number of traffic injuries for children in the recent years, motor vehicle crashes (MVCs) are still the leading cause of death for children from 3 to 14 years old (YO) in the United States. As reported in *Traffic Safety Facts, 2009 Data: Children* (National Center for Statistics and Analysis, 2010), in 2009, there were 1,314 traffic fatalities and 179,000 traffic injuries in children 14 and younger in the United States. Among these injuries, more than 50 percent occurred in frontal crashes, followed by about 25 percent in side impacts. Regardless of crash direction, head injuries are the most common serious injuries for children in MVCs.

To reduce head injuries for children, restraint systems and padding in rear seat compartments are both important. An effective restraint system could reduce the head excursion in an MVC, which will either avoid the head contacts to the vehicle interior or reduce the impact velocity if a head contact is unavoidable. Padding or an air bag, on the other hand, could attenuate the loads and accelerations applied to the head during a head contact, and in turn reduce the risk of head injury. In the recent child passenger safety research, much work has been done to improve the child restraint system for reducing the head excursions, especially in frontal crashes. However, to determine which areas and structures should be padded, and to identify the best deployment zone for a side curtain air bag, knowledge of likely child head impact locations for a range of crash scenarios is needed. Federal Motor Vehicle Safety Standard (FMVSS) No. 201, "Occupant protection in interior impact," issued by National Highway Traffic Safety Administration (NHTSA) requires vehicles 10,000 pounds or less to provide protection when an occupant's head strikes upper interior components such as pillars, side rails, headers, and the roof, but it does not include the vehicle interior area below the window sill. Similarly, curtain air bags generally do not cover the area below the window sill either.

Previous research on pediatric head contact locations in the rear seat has examined field data. Focusing on side-impact crashes, Maltese, Locey, Jermakian, Nance, & Arbogst (2007) extracted 24 cases of children 4 to 12 years old involved in side-impact crashes (principal direction of force [PDOF] 45 to 90 or 270 to 315 degrees) from the Crash Injury Research and Engineering Network and the Partners for Child Passenger Safety databases. All children were using lap or lap-shoulder belts without harness restraints or booster seats and each received at least an AIS 2+ injury. The investigators developed a head/face "contact location map" based on data available from crash investigations. The results showed a majority of the head contacts were in the rear half of the window and below the center of the window. More recently, Arbogast, Wozniak, Locey, Maltese, & Zonfrillo (2012) analyzed 28 cases of children ages 0 to 15 years old who were restrained in forward-facing child restraints, booster seats, or lap and shoulder belts and sustained AIS2+ head/face injuries in frontal crashes. A head contact location map was developed to summarize the vehicle components related to the causation of head injuries in children. The majority of the head/face contact locations were to the first row seat backs and B-pillars. The results from previous studies help to illuminate the types of injuries that children sustain in frontal and side-impact crashes and their association with contact locations, but crash-based data analyses with children are limited by small sample sizes and uncertainty about the crash characteristics and initial child positioning.

The objective of this study is to use a scalable MATHematical DYNAMIC MOdels (MADYMO) model of a child occupant to estimate the distributions of possible head impact locations as a function of crash direction, vehicle interior characteristics, and child size. To achieve this goal, 3D geometries of the second-row compartment from five vehicles were recorded by a laser scanner for use in assessing probable head contact zones. Simulations of crashes ranging from pure frontal to pure side impact (9 o'clock to 3 o'clock) with child anthropometric test device (ATD) models, with and without backless boosters. These were conducted using UMTRI's parametric child ATD model in MADYMO, UMTRI's child ATD positioning procedure, and UMTRI's automated belt-fit and crash simulation system. By combining the head motion model and the vehicle second-row geometry models, the likely head contact zones with respect to interior component were identified.

2 Methods

2.1 Vehicle Scan Procedure

In UMTRI's previous research, a FARO arm (Bronze Model, FARO Technologies, Lake Mary, Florida) coordinate digitizer was used to measure the interior geometry of ninety passenger vehicles. Seat, floor, roof and pillar surfaces shapes were outlined and then sampled in a grid pattern as shown in Figure 1. The H-point locations of the driver and rear-passenger seats were measured using the procedures in Society of Automotive Engineers (SAE) J826 as illustrated in Figure 2 (SAE, 2004). The fore-aft, up-down, and recline adjustment range of the seats were also measured. In the current study, a second FARO arm (Fusion Model) with a laser scanner was used to record more detailed surface information in five of these vehicles (Figure 3). The scan data were processed using reverse engineering software (Geomagic Studio 12). The data processing steps included creating polygonal meshes from the laser scan point cloud, cleaning of the scan surface to reduce noise, and reducing the number of polygons per vehicle to approximately 200,000.



Figure 1: FARO arm shown mounted to a vehicle (left) and being used to digitize the shape of vehicle pillar (right) in a grid pattern.



Figure 2: Measuring the location of the rear seat H-point



Figure 3: Fusion FARO arm with laser scanner attached

2.2 ATD Model Development and Validation

In this study, a parametric child ATD MADYMO model previously developed by Wu, Hu, Reed, Klinich, & Cao (2012) was used to conduct all simulations. This model can represent 6- to 12-year-old children and has been calibrated and validated against 12 sled tests with standard Hybrid III (HIII) 6- and 10-year-old child ATDs, two cushion lengths with realistic vehicle seats, and three seat belt anchorage configurations (Klinich, Reed, Ebert, & Rupp, 2011). The baseline version of this parametric model is shown in Figure 4. The standard abdomen and pelvis geometries of the original MADYMO 6-year-old child ATD model were refined by adding more detailed ellipsoids and facet meshes. To scale the baseline child ATD model into different body sizes, custom software was developed by combining MADYMO Scaler and a program written in Scilab V5.2.2, an open source numerical computational package. The scaling was based on the anthropometric data of children from 2 to 12 years old available in the GEnerator of BOdy Data (GEBOD) database (Cheng, Obergefell, & Rizer, 1996), which was derived from the study by Synder, Schneider, Owings, Reynolds, Golomb & Schork, 1977. The resulting models represent the average child attributes for children of each age.

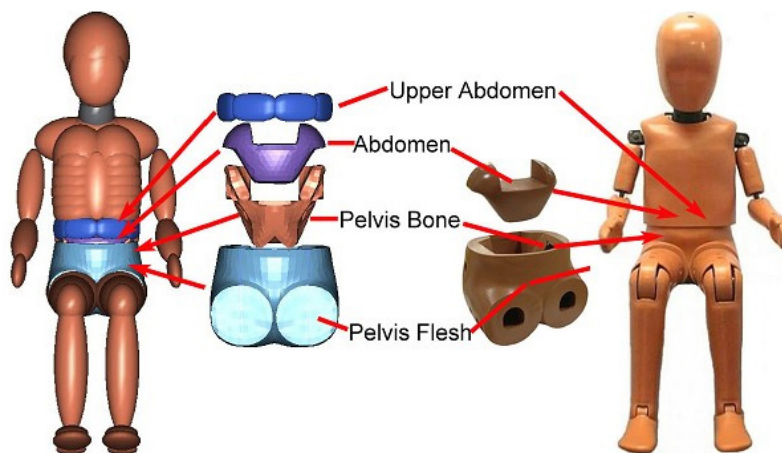


Figure 4: Baseline Hybrid III 6YO ATD model (Wu et al., 2012)

A second-row captain's chair model from 2008 Dodge Caravan was used in this study. Figure 5 shows the comparison between the underside of the real seat cushion and the seat cushion model. Facet elements constructed from scan data were used to obtain accurate geometry of the foam surface of the seat cushion. The supporting structures underlying the cushion were modeled by two cylinders. The front column was used to represent the steel frame at the front edge of the cushion, and the rear column was used to represent the two steel bars and the elastic webbing under the cushion foam. The contact characteristics of the seat cushion and the rear column of the seat structure were calibrated against data from 12 sled tests (Klinich, Reed, Ebert, & Rupp 2011; Wu, Hu, Reed, Klinich, & Cao, 2012), and the front column of the seat structure was defined as rigid. A generic backless booster seat was also used in this study to estimate the head motions from children seating in a backless booster seat.

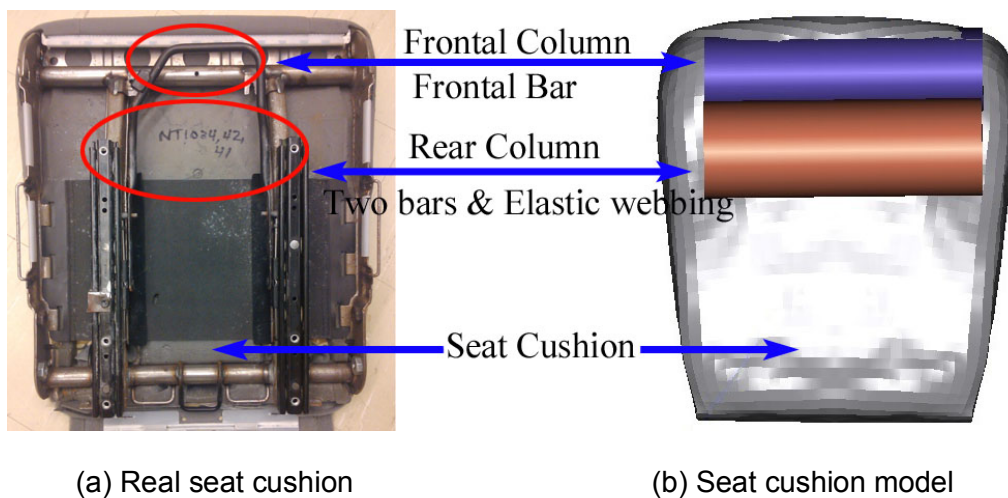


Figure 5: Comparison between real seat cushion and seat cushion model (bottom view).

The ATD position and seating posture were determined by the ATD stature and seat cushion length using a regression model developed by Reed, Ebert & Flannagan (2013). This seating posture model is based on child volunteer tests in realistic vehicle seating environments, thus providing a better representation of children's slouching posture caused by the relatively long seat cushion compared to their short thigh length. In the current study, the hip and head center of gravity (CG) points were used as the reference points to position the ATD. When a booster was used, the seating posture model considered the length of the booster seat as the length of the seat cushion. Figure 6 shows the postures of children at different ages seated in the same vehicle seat and booster seat after using these procedures.

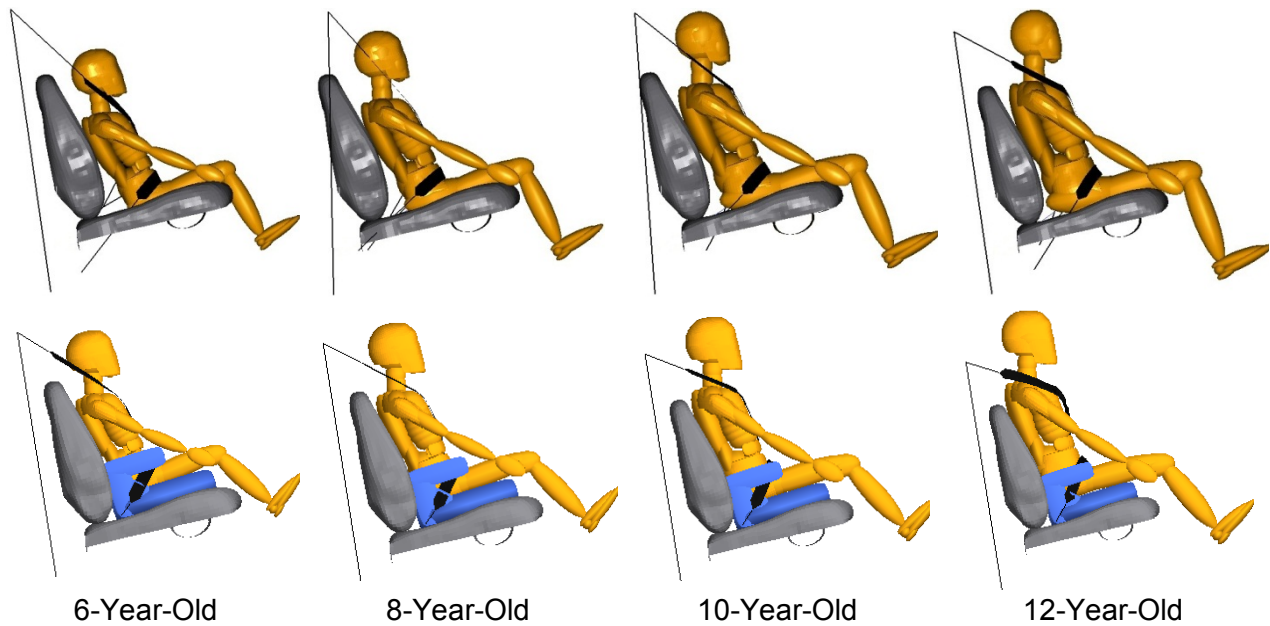


Figure 6: Seating postures of ATDs with different body sizes in vehicle seat and booster

2.3 Crash Conditions

To set up the crash simulations that properly reflect the real-world crash scenarios, the distributions of longitudinal and lateral delta V in crashes from the National Automotive Sampling System – Crashworthiness Data System (NASS-CDS) database were identified. The dataset used contains the NASS-CDS cases from 2006 to 2010 that include estimates of lateral and longitudinal delta V. The 19 cases in which the ratio inflation factor (commonly known as NASS sample weighting) was greater than 6,000 were deleted. Vehicle model years older than 2001 were deleted to achieve consistency across case years with data collection strategies implemented in 2010. The resulting dataset had 8,418 cases, weighted to 2,690,469 cases. All analyses used weighted data. Data were grouped into general crash directions using PDOF expressed as a clock direction as frontal (11-12-1), right-side (2-3-4), rear, (5-6-7), and left-side (8-9-10) crashes.

The distribution of crashes by PDOF is shown in Figure 7, and the delta V percentiles are shown in Table 1. In the current study, the maximal longitudinal delta V of 40 km/h and maximal lateral delta V of 36 km/h (Figure 8) were used in the simulations, which are close to the 95th percentile delta V in each direction. The simulated delta V from the PDOF of 3 o'clock through 12 o'clock to 9 o'clock are shown in Figure 8, in which an ellipse equation was fit using the semi-major axis of 40 km/h and semi-minor axis of 36 km/h. To determine the crash pulse with a specific delta V and crash angle, crash pulses generated by Side-NCAP and FMVSS No. 214 side-impact tests from five vehicles were analyzed, and an approximate crash pulse scalable for simulating different delta V was generated.

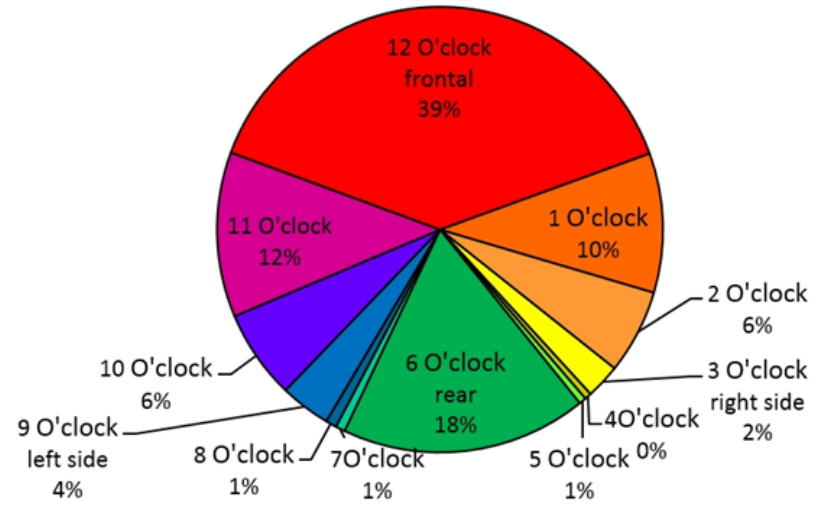


Figure 7: Distribution of crashes by PDOF. Numbers indicate clock direction and percentage of all planar crashes.

Table 1: Key percentiles value of delta V (km/h) for each crash mode.

Percentile	Total Delta V			
	Frontal 11,12,1 o'clock	Right 2,3,4 o'clock	Left 8,9,10 o'clock	Rear 5,6,7 o'clock
50	18	17	16	16
75	25	24	22	21
80	28	26	23	23
90	34	31	29	27
95	40	37	34	34
98	47	43	41	42
99	55	49	45	46

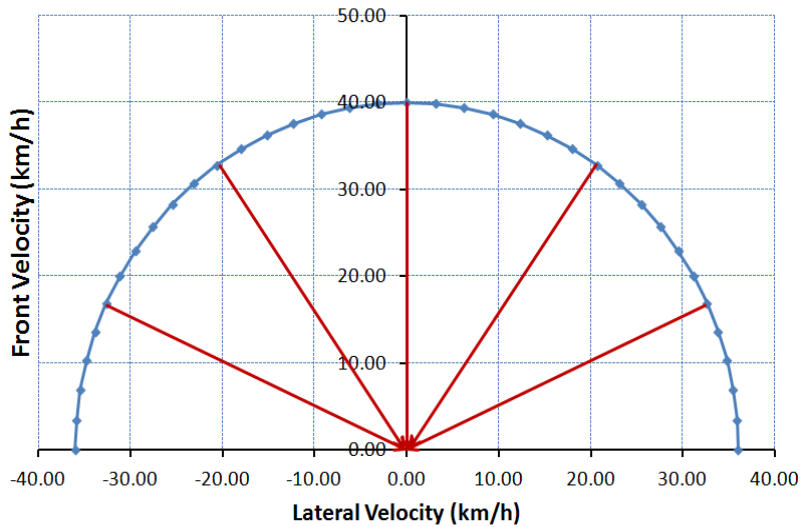


Figure 8: Simulated delta V

2.4 Simulation Matrix

In this study, 1,000 simulations were performed using a booster-seat model and 1,000 without the booster. The simulation matrix was generated using the Uniform Latin Hypercube method, which produced even distributions for the input variables and covariates. Table 2 summarizes the range and mean of the variables of the parametric study in 1,000 simulations. Input variables (e.g., impact angle) are those whose effects were monitored. Covariates (e.g., belt anchorage locations) were included to introduce the effects of factors known to vary in the simulated scenarios, but the effects of covariates were not monitored. The range of seat belt anchorage locations selected in this study were based on a large range of vehicle seat and belt configurations reported by a survey of second-row seating positions in late-model vehicles (Reed, Ebert-Hamilton, Manary & Rupp, 2008) that are within the allowable locations specified by FMVSS No. 210. The range of cushion length was obtained by measuring a sample of second- and third-row cushion lengths of 56 late-model vehicles (Huang & Reed, 2006; Klinich, Reed, Ebert, & Rupp, 2011). The position of the front column of seat structure relative to the seat cushion was the same for all cushion lengths, while the position of the rear column of the seat structure was obtained by linear interpolation from two validated seat models with long and short cushions. In real vehicles, the seat belt inboard and outboard anchors are often designed to achieve similar lap belt angles on both sides. Therefore in this study the two lap belt anchorages were moved forward and backward simultaneously.

Table 2: Distributions of variables in the parametric study

	Variables	Unit	Lower Bound	Upper Bound	Mean	Reference	
Input Variables	Impact Angle	Deg	-90	90	0		
	Longitudinal Delta V	Km/h	0	40	20		
	Lateral Delta V	Km/h	-36	36	0		
	Age	-	6	12	9		
Covariates	D-Ring	X	mm	-550	-250	-400	Coordinates in reference to the H-point of the seat as the origin; X+ forward, Y+ inward and Z+ upward.
		Y	mm	-300	-200	-250	
		Z	mm	475	700	588	
	Outboard Anchor	X	mm	-300	-50	-175	
		Y	mm	-320	-150	-235	
		Z	mm	-325	-75	-200	
	Inboard Anchor	X	mm	-250	-25	-138	
		Y	mm	140	275	208	
		Z	mm	-235	-90	-163	
	Cushion Stiffness	%	50%	150%	100%	The real vehicle seat (Wu et al., 2012)	
Seat Supporting Structure Vertical Location	mm	-15	15	0			
Cushion Length	mm	350	500	425	Huang et al., (2006)		
Output Variables	Head Top Trajectory	Curves				Coordinates in reference to the H-point of the seat as the origin; X+ forward, Y+ inward and Z+ upward.	
	Head CG Trajectory	Curves					
	Left Shoulder Trajectory	Curves					
	Right Shoulder Trajectory	Curves					
	Left Knee Trajectory	Curves					
	Right Knee Trajectory	Curves					

2.5 Automated Simulation Procedure

An automated simulation procedure was developed to enable this large-scale study. In the current study, simulations were conducted using modeFrontier (a multi-objective optimization and design environment) coupled with MADYMO (a software package for the analysis of occupant safety systems in the automotive industry) and Scilab (an open source numerical computational package). Figure 9 shows the flowchart of setting up a single simulated iteration. First, the age of the child occupant was input, and the corresponding weight and height were determined based on 50th percentile values provided by the CDC child growth chart. The ATD model was generated based on the age, weight, and height using MADYMO Scaler and Scilab following the procedure described above. Once the ATD model was generated, it was positioned according to the UMTRI seating posture model based on the seat cushion length and reference stature. A MADYMO pre-simulation was then conducted to pull the seat belt, so that it closely fit the body contour of the child occupant. If a booster seat was present, the lap belt guides of the booster were initially rotated away from the belt path during the pre-simulation to better predict the belt location. Once the pre-simulation is done, the resulting estimated occupant posture and belt position were input into the final MADYMO simulation along with the crash pulse predicted based on the impact angle. Each crash simulation generally took less than 2 minutes. A Scilab program was written to extract the MADYMO results, so that the trajectories from different body regions can be displayed.

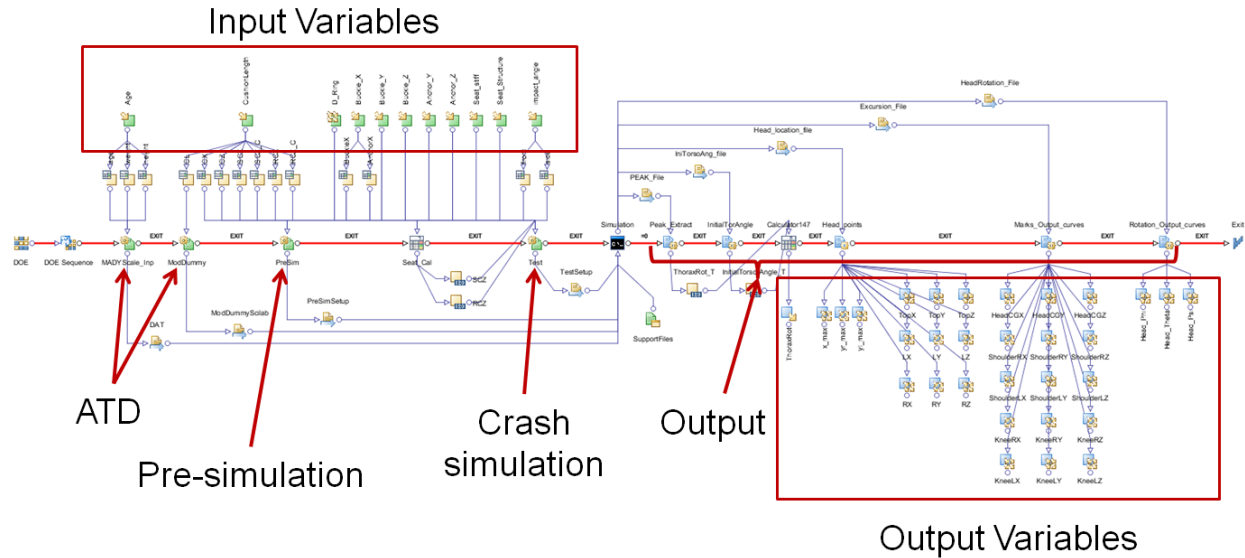


Figure 9: ModeFrontier flowchart for setting up the automated simulations

2.6 Head Contact Zones

The head contact zones were achieved by overlaying the trajectories of the head top of child ATDs in crashes and the vehicle second-row environment geometry. The reference point for both head trajectories and vehicle geometry is the H-point of the second-row seat behind the driver seat. Intersection between the head trajectories and the vehicle second-row geometry indicates a potential contact location.

3 Results

3.1 Vehicle Scans

Five vehicles, including three sedans (Audi A4, Mazda 6, and Toyota Corolla), one Sport Utility Vehicles (SUV) (Saturn Vue), and one minivan (Toyota Sienna) were scanned. Figure 10 shows the scanned second-row environment geometry. Each vehicle was represented by approximately 200,000 triangle elements. In each case, all the seats, if adjustable, were measured and represented in its full-rear, full-down position, with the seat back angle (SAE A40) set to 22 degrees.

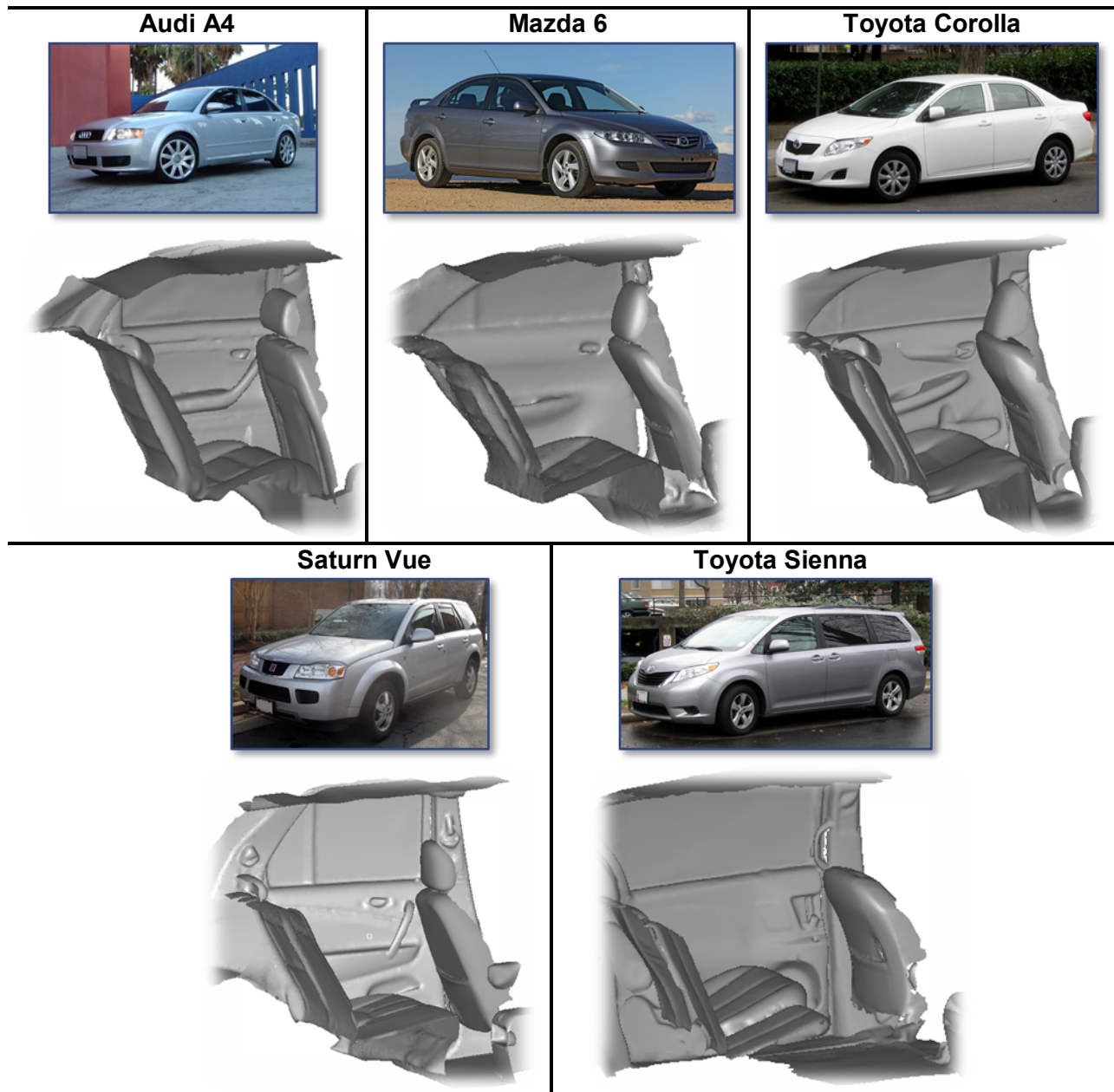


Figure 10: Scanned vehicle second-row environment geometry

3.2 Vehicle Crash Pulse

Crash pulses from Side-NCAP and FMVSS No. 214 side impact tests for five vehicles, including the 2004 Toyota Camry, 1999 Dodge Caravan, 2010 Dodge Journey, 2010 Ford Taurus, and 2009 Honda Accord, were compared. Figure 11 shows the comparison, in which three trends are fairly clear. First, the pulse shapes between the Side-NCAP and FMVSS No. 214 tests are very similar. Second, the maximal accelerations of Side-NCAP pulses are consistently higher than those from the FMVSS No. 214 tests, while the duration of the pulse did not change much. Third, the delta V of Side-NCAP tests were 5-10 km/h higher than those in the FMVSS No. 214 tests. Therefore, in this study, the crash pulse was scaled based on delta V without changes in the pulse duration.

Following this approach, the crash pulses in FMVSS No. 214 tests for the five vehicles in Figure 8 were scaled to the ones corresponding to a delta V of 38 km/h. The midline of the crash pulse corridor of FMVSS No. 213 test (frontal crash) was also scaled down to 38 km/h, and was compared to those scaled side impact crash pulses in Figure 12. The scaled real vehicle side impact crash pulses were markedly similar to the scaled FMVSS No. 213 crash pulse, indicating that we could use one baseline crash pulse and decompose it into frontal and lateral pulses to simulate the oblique crash conditions. In the current study, the midline of FMVSS No. 213 crash pulse corridor was used as the baseline crash pulse for all simulations.

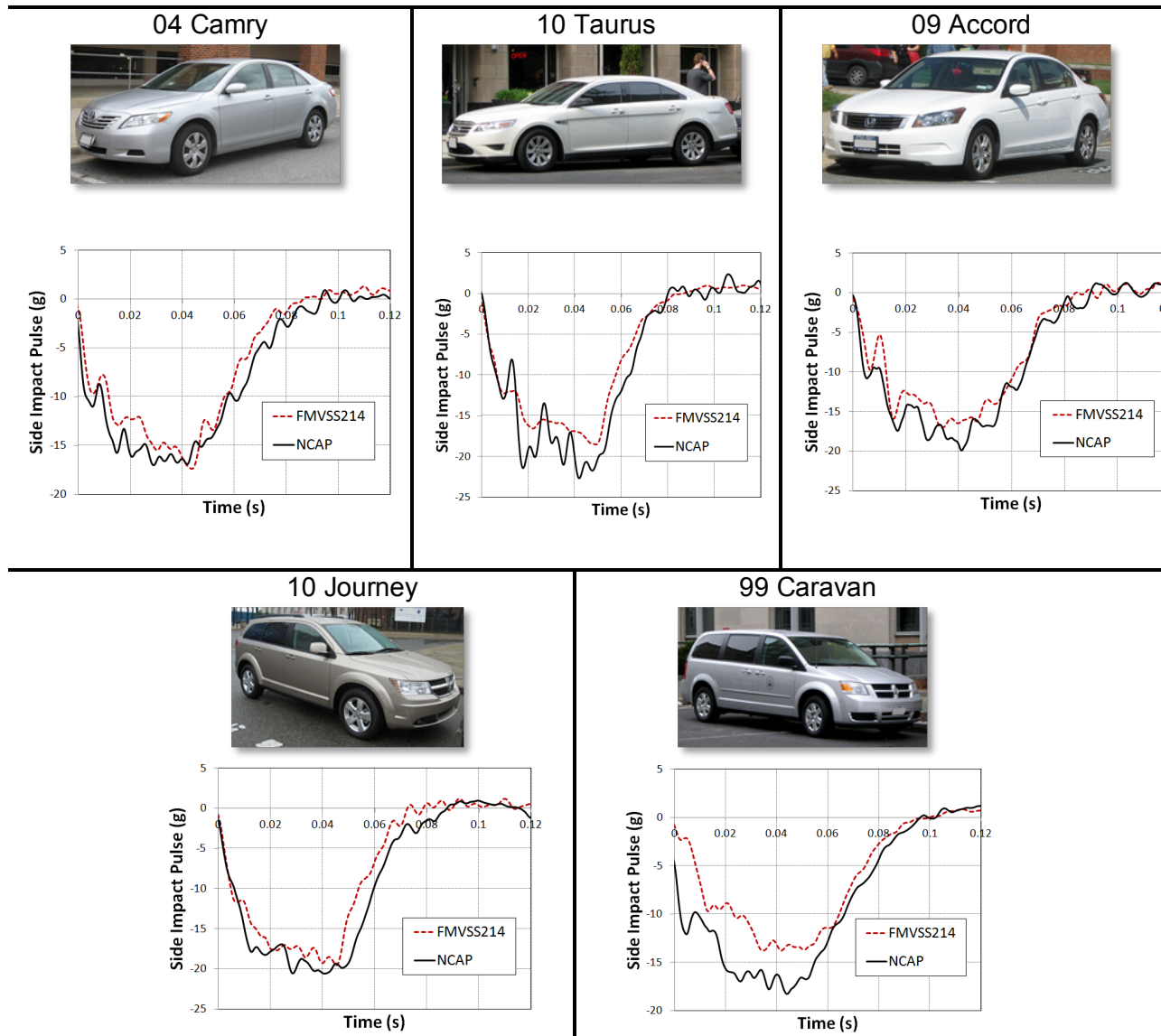


Figure 11: Comparison of crash pulses between Side-NCAP and FMVSS No. 214 side impact tests

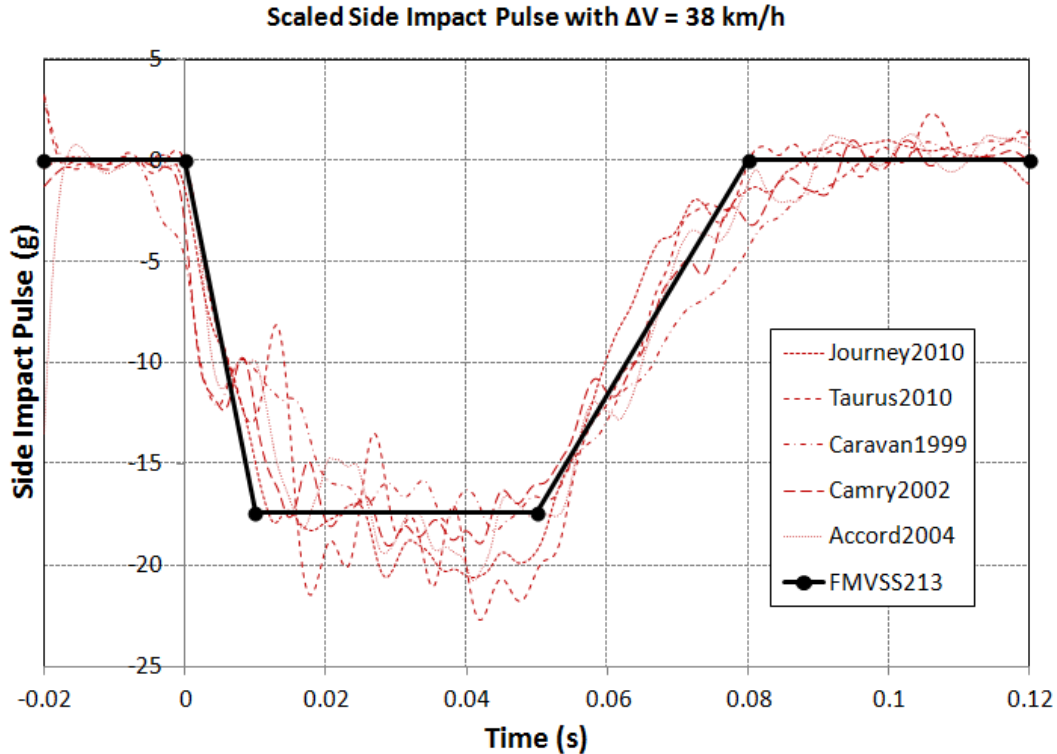


Figure 12: Comparison of scaled crash pulses between FMVSS No. 213 test and vehicle side impact tests FMVSS No. 213 curve presents the center of the crash pulse corridor

3.3 Simulated Head Trajectories Compared to Vehicle Second-Row Geometry

Figure 13 shows the head top trajectories for the 6-, 9-, and 12-year-old ATD models with and without boosters. Stature is a dominant factor in determining the head trajectory, as larger statures were associated with higher head excursions, in turn increasing the possibility of head contact. In general, the seat belt performed the best in limiting the head excursions in frontal crashes, followed by the near-side impacts. The largest excursions were observed in far-side impacts. Booster seats elevated the head initial position, but did not change the head forward or near side excursions. However, the booster seat showed the potential to increase the head excursions in far-side impacts.

To facilitate the interpretation of the head trajectories, seat back location quantiles from a related analysis (Wu, Hu, Reed, Klinich, & Cao, 2012) were included. These quantiles are based on an analysis of data from 50 vehicles that included consideration of the distribution of driver seat positions based on driver stature. As an example of the interpretation of these curves, 90th percent of driver seats, across vehicles, are expected to be positioned closer to the second-row H-point than the 10th percentile curve.

Figure 13 shows that ideally positioned 6-year-old child ATD are not likely to contact the front seat back, because their head top trajectories did not intersect with the seat at the 99th percentile rearward location. However, the simulated head trajectories intersected the 95th

percentile curve for the 9-year-old body size, and the trajectories for the 12-year-old body size reached as far as about 80th percentile seat position curve.

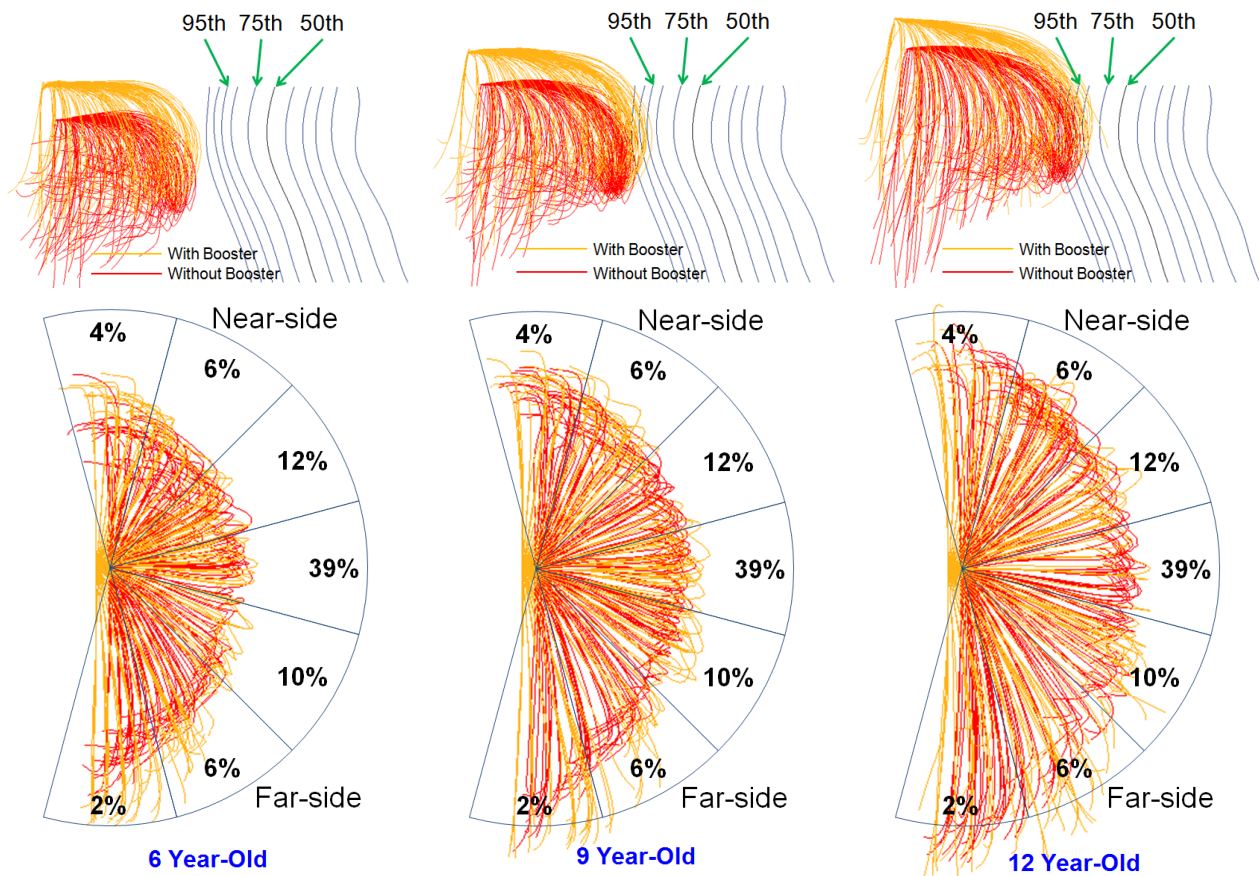


Figure 13: Head top trajectories of simulated child ATDs with and without booster seats.

Pictures in the first row are from the side view, in which head trajectories are overlaid with quantiles of the front seat back locations (Reed, Ebert, & Klinich, 2014). Pictures in the second row are from the top view, in which the distribution of the PDF highlights the research priorities

Tables 3 to 5 show the head top trajectories of child ATD models with and without booster seats overlaid in the second-row geometries in the Audi A4, Toyota Sienna, and Saturn Vue. These vehicles represent passenger cars, minivans, and SUVs, respectively. Overall, larger body size was associated with an increased possibility of contacting the back of the front seat and side interior. However, the three vehicles showed very different second-row geometry in terms of the 3-dimensional space relative to the head trajectories.

Audi A4, as a mid-size passenger car, has a relatively small fore-aft space for the second-row, when the front seat is in the most rearward position. The most rearward position of the front seat of Audi A4 places it near the 95th percentile position of predicted driver seat positions across all vehicles measured (taking into account a wide range of driver stature). Based on the simulation results, when seated directly on the vehicle seat without a booster, the head of the 6-year-old ATD model may contact the rear-portion of the door interiors below the window sill of the Audi A4. The head-to-side-door contact locations for 9-year-old ATD were slightly above the window

sill, and the contact locations for the 12-year-old ATD model were around the rear-middle portion of the door window. As for child ATDs with booster seats, the head-to-door contact locations shifted above those without booster seats by about the height of the booster. As a result, the head contact locations are generally above the window sill for 6- to 12-year-old ATD models. In this study, the height of a 12-year-old ATD was assigned as 1,506 mm, which is the median height of 12-year-old children based on the CDC growth chart. Based on our simulations, using a booster with this height may lead to a head-to-roof contact before contacting the door based on our simulations. However, the current study did not simulate any sort of slouching or spine flexion. Realistically, if a 12-year-old child uses a booster seat, spine flexion would exist at levels beyond that included in the models, which will significantly reduce the possibility of head-to-roof contacts.

As a minivan, the Toyota Sienna showed great space in the second-row, partially due to the fact that the vehicle geometry scan was taken while all seats were in the most rearward positions, including the second-row seats. For the Sienna, the most rearward position of the front seat locates around the 1st percentile rearward position. Consequently the head top trajectories predicted by the 6- to 12-year-old ATD models were all far from the back of the front seat for Sienna. Comparing to Audi A4, Sienna has a relatively wider vehicle space and lower window sill. As a result, the simulated head-to-door contact locations for 6- to 12-year-old ATDs are generally on or above the window sill in side or oblique impacts. However, because the second-row seat was positioned at the most rearward location in this study, the simulation results showed the potential for the heads of 6- to 12-year-old ATDs to contact the C-pillar.

As an SUV, the Saturn Vue's second-row space is larger than the Audi A4, but smaller than the Toyota Sienna. The most rearward position of the Vue's front seat locates near the 80th percentile rearward position of the rear seats measured. Consequently, 12-year-old ATD may contact the back of the front seat based on the simulation results, but not the 6- or 9-year-old ATDs. However, the Saturn Vue also showed some geometry features distinct from Audi A4 and Sienna. In particular, Vue's window sill is relatively higher than those from Audi A4 and Sienna, and its C-pillar is located in a relatively more forward location. These geometry features may result in head contacting the door below the window sill (especially for ATDs smaller than 9-year-old without booster seats) and the C-pillar (especially for ATDs bigger than 9-year-old with booster seats).

The above results clearly showed that child body size and vehicle compartment size both affected the possibility and location of a head contact in motor vehicle crashes.

Table 3: Head top trajectories of child occupants with (yellow) and without (red) booster seats overlaid in the Audi A4 second-row geometry

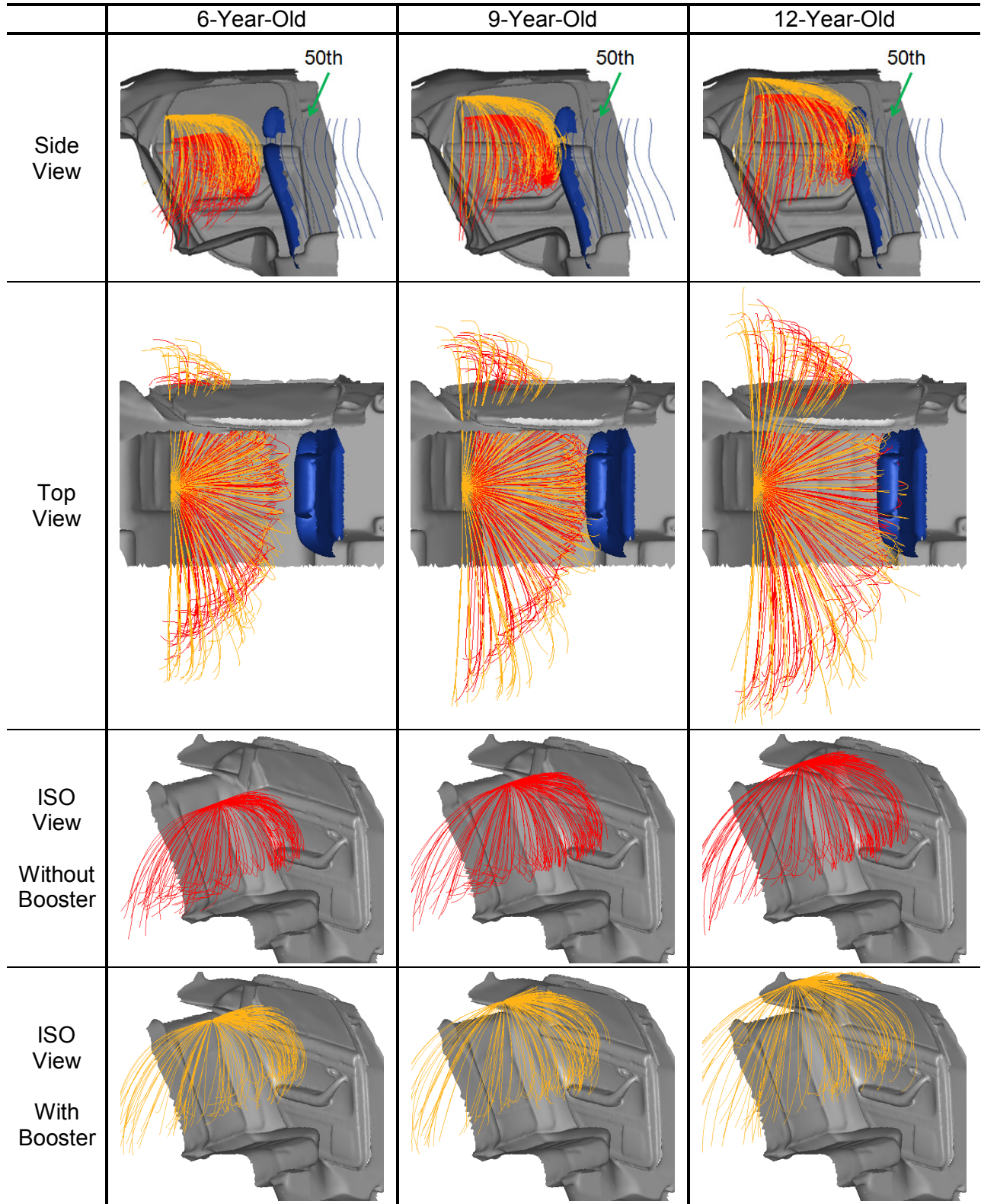


Table 4: Head top trajectories of child occupants with (yellow) and without (red) booster seats overlaid in the Toyota Sienna second-row geometry

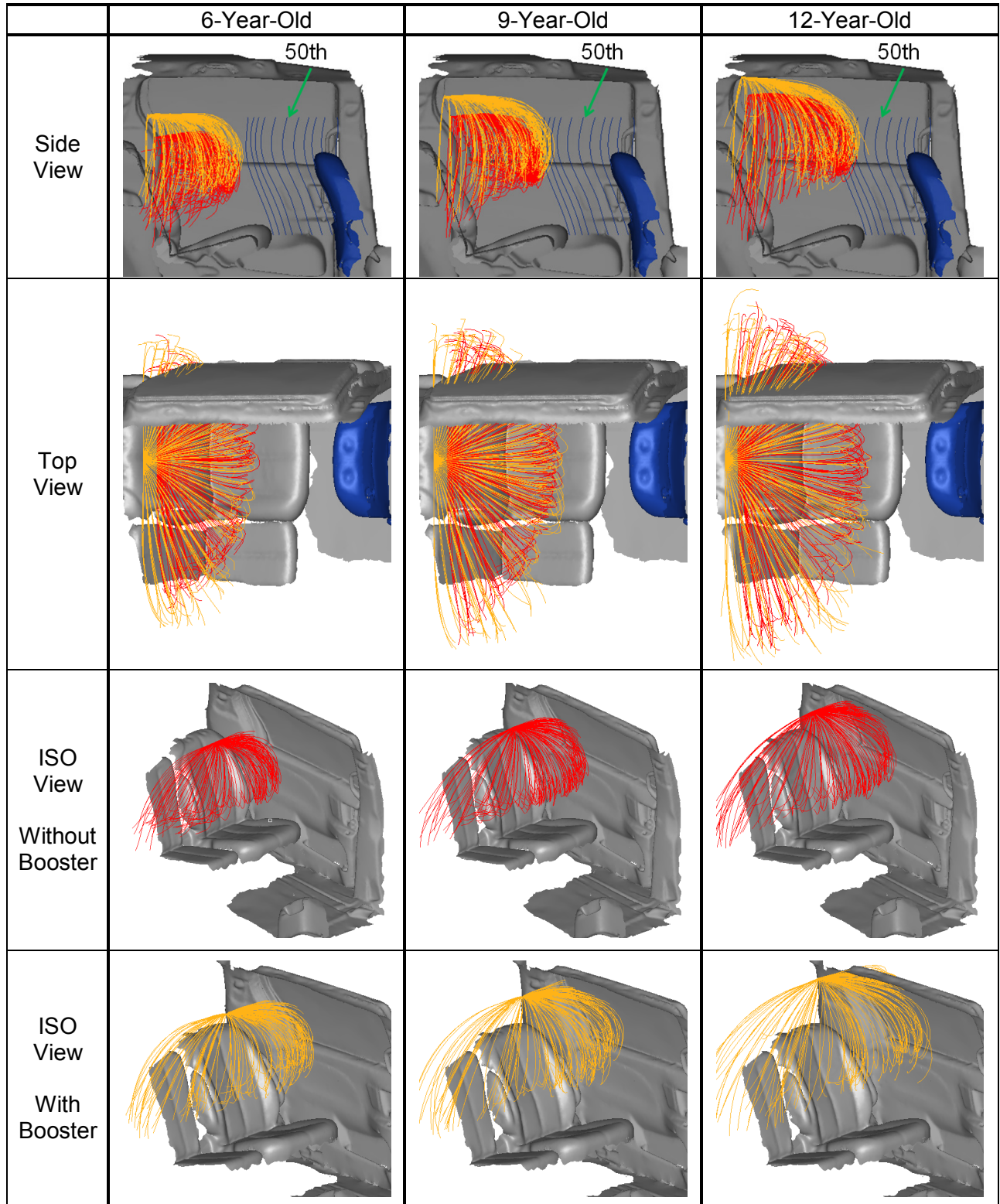
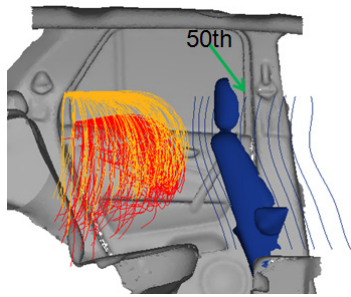
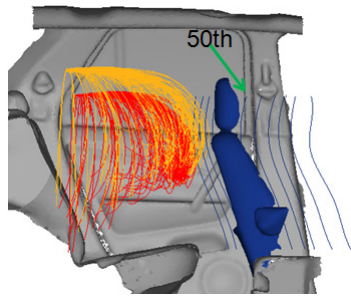
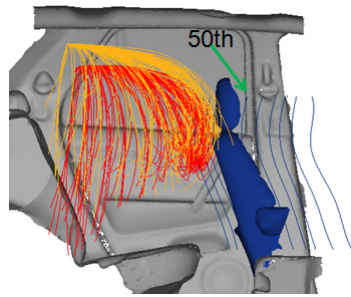
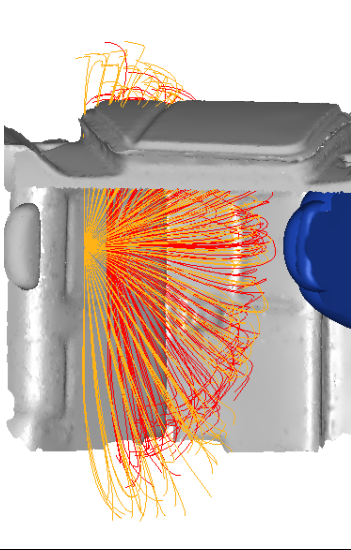
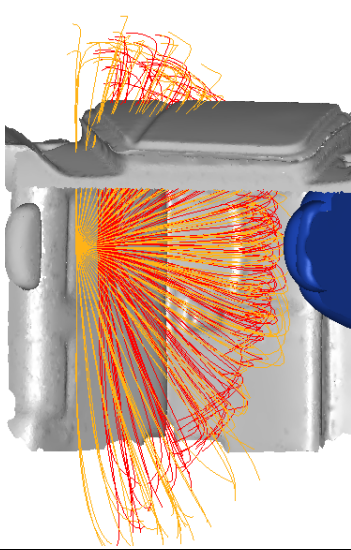
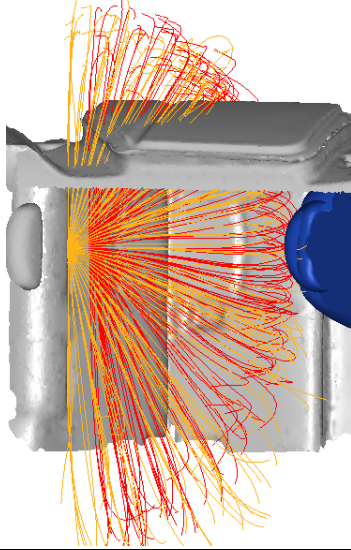
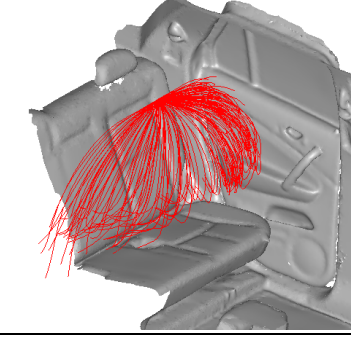
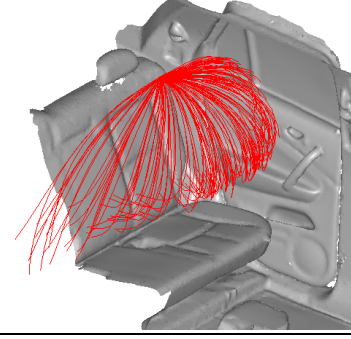
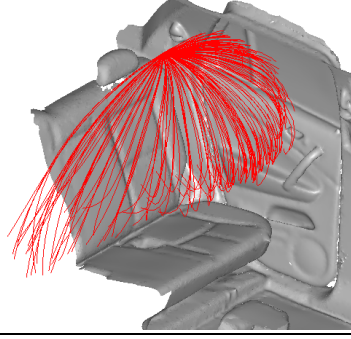
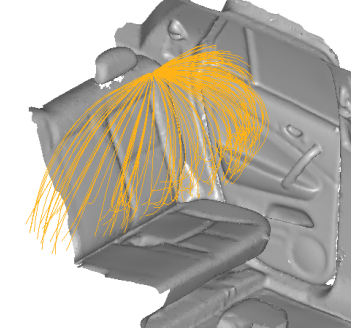
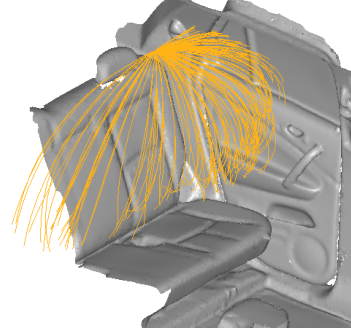
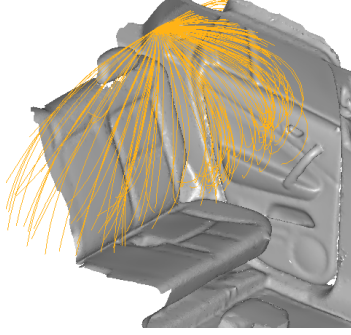


Table 5: Head top trajectories of child occupants (yellow) and without (red) booster seats overlaid in the Saturn Vue second-row geometry

	6-Year-Old	9-Year-Old	12-Year-Old
Side View			
Top View			
ISO View Without Booster			
ISO View With Booster			

3.4 Head Trajectory as a Function of Delta V

Figure 14 shows the typical head top trajectories of 6-, 9-, and 12-year-old child ATDs at delta V from 20 to 60 km/h with an interval of 5 km/h. The typical head top trajectories were calculated based on 300 simulations with crash direction within $\pm 5^\circ$ of the pure frontal direction using a multivariate regression analysis. The results suggest clear effects of body size and delta V on the head trajectories of child ATDs with 12-year-old ATD contacting about 60th percentile front seat line at 60 km/h and 99th percentile at 35 km/h.

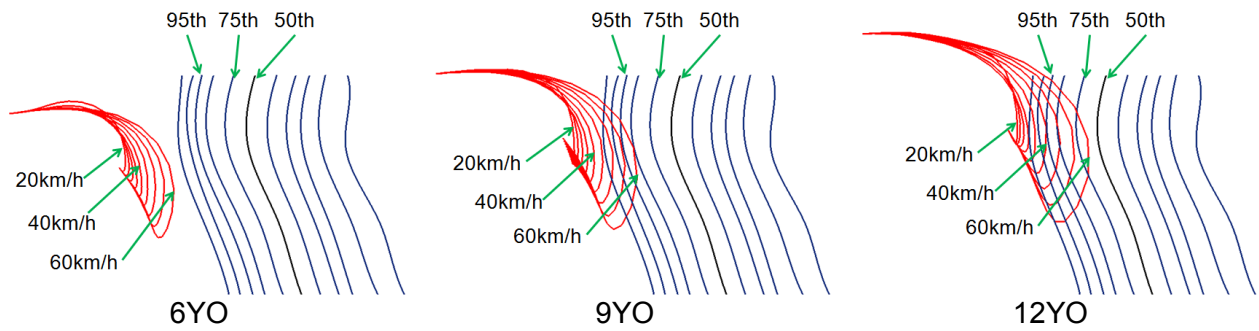


Figure 14: Head top trajectories of simulated child ATDs with different delta V

4 Discussion

Unlike previous crash-based data analyses for children, the research work presented in the current study is the first to use computational simulations to predict head contact zones for 6- to 12-year-old children in frontal, side, and oblique impacts for rear seat environments. As the crash-based data analyses with children are limited by small sample sizes, automated computational study enabled large sample size and allowed a systematic investigation of possible head impact locations for older children as a function of crash type, vehicle interior characteristics, child size, and use of booster seats.

4.1 Comparing to Previous Studies in terms of Head Contact Zones

Figure 15 shows a comparison of the head contact zones in side impacts reported by Maltese, Locey, Jermakian, Nance, and Arbogast. (2007) based on 24 cases and those predicted in the current study based on computational simulations. In general, they are very consistent, and the majority of the head contact locations were found horizontally within the rear portion of the window and vertically within the lower portion of the window. However, due to the nature of computational simulations, the current study allowed the effects of vehicle type and child size to be analyzed more systematically. The simulations indicated that normally seated (without booster) 6- to 8-year-old children may be more likely to contact the side interior below or on the window sill, especially in SUVs, which generally have high window sill relative to the seat. In contrast, the larger body size of 9- to 12-year-old children may make them more likely to contact the window above the window sill in side impacts.

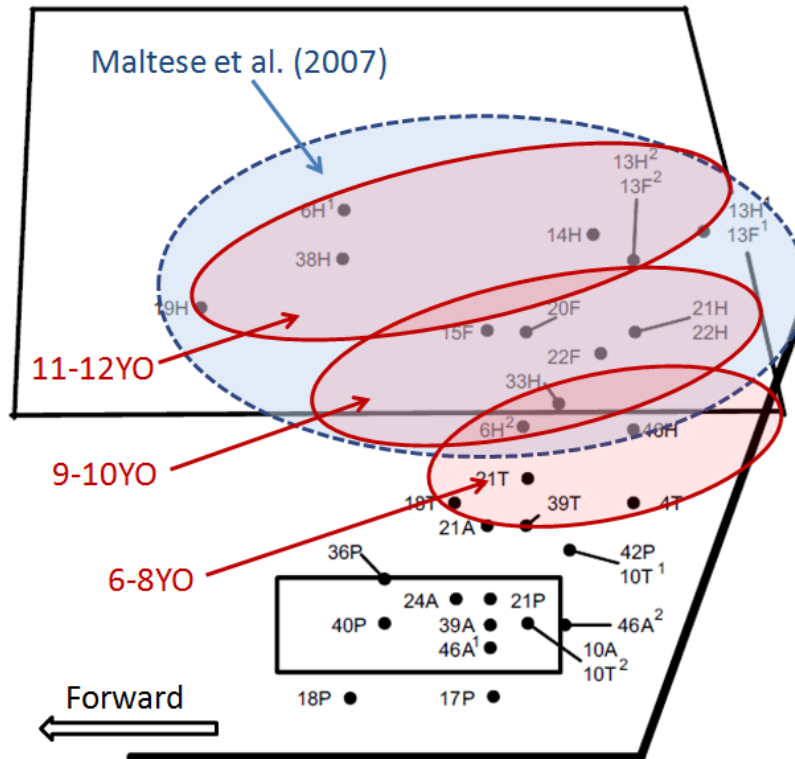


Figure 15: Comparison of head contact zone between the Maltese study and simulated contacts for 6- to 8-, 9- to 10-, and 11- to 12-year-old children in the current study

As for frontal crashes, Arbogast, Wozniak, Locey, Maltese, & Zonfrillo (2012) reported that the most common contact zone for left rear child occupants in 21 crashes with child head/face injuries was on the B-pillar, while the most common contact zone for right rear child occupants was on the passenger's seat back. The simulations of ideally positioned children in the current study did not produce head contact with the B-pillar regardless of age, crash direction, or vehicle type. These findings suggest that B-pillar contacts may be due to more-complex crash kinematics, belt slack, different initial postures or positions, or other factors not reflected in these simulations.

4.2 Seat Belt and Booster Seat Effectiveness in Reducing Injuries for Children

Even though the effectiveness of the seat belt in reducing injuries in motor vehicle crashes has been well documented (Cummings, Wells, & Rivara, 2003), belts are less effective for children who are substantially smaller than adults. Children who use the vehicle belt prematurely may result in increased risk for serious injuries in crashes (Durbin, Elliott, & Winston, 2003; Arbogast, Kallan, & Durbin, 2005) due to either a bad belt fit (Reed, Ebert-Hamilton, Manary & Rupp, 2008) or belt misuse. Seat belts themselves can cause injuries, especially to the abdomen for young school-aged children due to "submarining," which is commonly referred to as "seat belt syndrome" (Tso, Beaver, & Haller, 1993; Durbin, Arbogast, & Moll, 2001; Arbogast, Chen, Nance, Durbin, & Winston, 2004; Santschi, Echave, Laflamme, McFadden, & Cyr, 2005; Stacey, Forman, Woods, Arbogast, & Kent, 2009). To improve the belt fit and reduce the likelihood of

belt misuse, booster seats are recommended by NHTSA for children who cannot fit properly in the vehicle belt.

In the current study, the potential effects of one backless booster seat model on head trajectories in severe crashes were examined. Other potential effects of boosters, such as reducing the risk of abdomen injuries, were not considered. Our results also showed that booster seat had only small effects on head trajectories. However, this finding is based on simulations in ideal seating positions, with the torso portion of the belt often placed very close to the neck. Variation in belt position due to child posture would be expected to affect the head excursion, although those effects were not investigated in these simulations. Boosters may also increase the likelihood that a child is properly positioned with respect to the belt, but that factor was not investigated in this study.

4.3 Implications for Vehicle Countermeasures

The results of this study suggest that head contact with the vehicle interior on the back of the front seats and on the door below the window sill can be expected for children who are using the vehicle belt for primary restraint without booster seats. In some vehicles, and with some front seat positions, a well-positioned child might not contact the front seat. But the simulations suggest that in many other conditions, particularly with taller children in smaller vehicles, head contact with the front seat can occur even when the child and belt are optimally positioned (i.e. shoulder belt in the middle of the shoulder and lap belt on the thigh). For lateral impacts, head contact below the window sill can occur, particularly for smaller children without booster seats. There is variation in window position with respect to the seat H-point, and hence with respect to the head locations of children. Vehicle designers could consider positioning countermeasures relative to the seat in addition to the window geometry, to increase the likelihood that children's heads contact the countermeasures without use of a booster seat.

4.4 Limitations and Future Work

There are several limitations in this study. The simulations were conducted using a MADYMO model of the Hybrid-III ATD, i.e., a computational model of a physical model of a child. The scaling of the model accounts for overall size, but does not incorporate the large range of variance in body size with age. The ATD model has been only validated in frontal crashes without booster seats with a single crash severity. Its validity in side, oblique, and frontal crashes with a booster seat needs further investigation.

All simulations were performed without any ATD-to-interior contact. Torso-to-interior contacts occurring before the head contact may change the head trajectory, although the similarities between the contact areas obtained by intersecting the trajectories with vehicle geometry and those documented in previous studies of child head/face injuries suggest that the results are reasonable. Because no head contact was simulated, the results cannot be used to infer injury risk.

Importantly, all simulations were performed using an ideally positioned child ATD model with no belt slack. Many possible alternative postures, and more realistic levels of belt slack, would tend to increase head excursion, except that conditions that produced submarining would tend to reduce head excursion. Because a single, backless booster condition was simulated, the results do not indicate whether alternative booster designs might have positive or negative effects on the risk of head contact.

5 Summary

This study used a scalable MADYMO model of a child occupant to estimate the distributions of possible head impact locations as a function of crash type, vehicle interior characteristics, and child size. The geometries of the second-row compartments of five vehicles were recorded with a laser scanner to provide high-resolution data for use in assessing head contact zones. Distributions of lateral and longitudinal delta V were calculated as a function of PDOF using the NASS-CDS dataset to provide proper simulation conditions based on real-world crashes. Simulations of crashes ranging from pure frontal to pure side impact (9 o'clock to 3 o'clock) with child ATDs with and without backless boosters were conducted using UMTRI's parametric child ATD model in MADYMO, UMTRI's child ATD positioning procedure, and UMTRI's automated belt-fit and crash simulation system. The simulation results were used to create a model of the spatial distribution of head trajectories based on child body size and crash direction. By combining the head motion model and the vehicle second-row geometry models, the likely head contact zones with respect to interior components were identified. The findings of this study provided a reference for future vehicle rear compartment design to reduce head injuries for children.

6 References

- Arbogast, K. B., Chen, I., Nance, M. L., Durbin, D. R., & Winston, F. K. (2004). Predictors of Pediatric Abdominal Injury Risk. *Stapp Car Crash J* 48: 479-494.
- Arbogast, K. B., Kallan, M. J., & Durbin, D. R. (2005). Effectiveness of high back and backless belt-positioning booster seats in side impact crashes. *Annu Proc Assoc Adv Automot Med.*;49:201-213..
- Arbogast, K. B., Wozniak, S., Locey, C. M., Maltese, M. R., & Zonfrillo, M. R.. (2012). Head impact contact points for restrained child occupants. *Traffic Inj Prev* 13(2): 172-81.
- Kahane, C. J. (2000, December). *Fatality reduction by safety belts for front-seat occupants of cars and light trucks: Updated and expanded estimates based on 1986-99 FARS data.* (Report No. DOT HS 809 199). Washington, DC: National Highway Traffic Safety Administration.
- Cheng, H., Obergefell, L., & Rizer, A. (1996). The development of the GEBOD program. In 15th Southern biomedical engineering conference, Dayton, OH, 1996, pp.251–254. New York: IEEE.
- Cummings, P., Wells, J. D., & Rivara, F. P. (2003). Estimating seat belt effectiveness using matched-pair cohort methods. *Accid Anal Prev* 35(1): 143-9.
- Durbin, D. R., Arbogast, K. B. & Moll, E. K. (2001). Seat belt syndrome in children: a case report and review of the literature. *Pediatr Emerg Care* 17(6): 474-7.
- Durbin, D. R., Elliott, M. R., & Winston, F. K. (2003). Belt-positioning booster seats and reduction in risk of injury among children in vehicle crashes. *JAMA* 289(21): 2835-40.
- Huang, S., & Reed, M. P. (2006). *Comparison of child body dimensions with rear seat geometry.* (Report No. SAE 2006-01-1142). Warrendale,PA: SAE International.
- Klinich, K. D., M. P. Reed, M. P., Ebert, S. M., & Rupp, J. D. (2012). *Effect of realistic vehicle seats, cushion length, and lap belt geometry on child ATD kinematics.* (Report No. DOT HS 811 869). Washington, DC: National Highway Traffic Safety Administration.
- Maltese, M. R., Locey, C. M., Jermakian, J. S., Nance, M. L., & Arbogast. KB. (2007). Injury causation scenarios in belt-restrained nearside child occupants. *Stapp Car Crash J* 51: 299-311.
- National Center for Statistics and Analysis. (2009). *Traffic safety facts 2009 data - children.* (Report No. DOT HS 811 387). Wahington, DC: National Highway Traffic Safety Administration.

- Reed, M. P., Ebert-Hamilton, S. M., Manary, M. A., & Rupp, J. D. (2008, September). *Assessing child belt fit, Volume I: Effects of vehicle seat and belt geometry on belt fit for children with and without belt positioning booster seats*. (Unnumbered NHTSA report. UMTRI Report No. UMTRI-2008-49-1). Washington, DC: National Highway Traffic Safety Administration. Available at <http://mreed.umtri.umich.edu/mreed/pubs/UMTRI-2008-49-1.pdf>
- Reed, M. P., Ebert-Hamilton, S. M., & Flannagan, C. A. C. (2013, November). Improving the repeatability and reproducibility of belt fit measurement with 6YO and 10YO ATDs. (Report No. DOT HS 811 857). Washington, DC: National Highway Traffic Safety Administration.
- Reed, M. P., Ebert-Hamilton, S. M., & Klinich, K. D. (2014, August). Characterizing vehicle rear compartment geometry for child restraint applications. (Report No. DOT HS 812 057). Washington, DC: National Highway Traffic Safety Administration.
- Santschi, M., Echave, V., Laflamme, S., McFadden, F., & Cyr, C. (2005). Seat-belt injuries in children involved in motor vehicle crashes. *Can J Surg* 48(5): 373-6.
- Stacey, S., J. Forman, Woods, W., Arbogast, K., & Kent, R.. (2009). Pediatric abdominal injury patterns generated by lap belt loading. *J Trauma* 67(6): 1278-83; discussion 1283.
- Synder, R. G., Schneider, L.W.; Owings, C.L.; Reynolds, H.M.; Golomb, D.H.; & Schork, M.A. (1977). *Anthropometry of infants, children, and youths to age 18 for product safety design*. Bethesda, MD: U.S. Consumer Product Safety Commission.
- Tso, E. L., Beaver, B. L., & Haller, J. A. Jr. (1993). Abdominal injuries in restrained pediatric passengers. *J Pediatr Surg* 28(7): 915-9.
- Wu, J., J. W. Hu, Reed, M. P., Klinich, K. D., & Cao, L. (2012). Development and validation of a parametric child anthropomorphic test device model representing 6-12-year-old children. *International Journal of Crashworthiness* 17(6): 606-620.

DOT HS 812 105
December 2014



U.S. Department
of Transportation
**National Highway
Traffic Safety
Administration**



11092-122314-v2